Design Space Exploration of Pericyclic Transmission with Counterbalance and Bearing Load Analysis

Zachary A. Cameron
Research Engineer
NASA Glenn Research Center
Cleveland, OH, USA

Dr. Edward C. Smith
Prof. Aersp. Engr.
Penn State University
University Park, PA, USA

Dr. Hans DeSmidt
Prof. Mech. Aersp. Engr.
University of Tennessee
Knoxville, TN

Dr. Robert C. Bill
Research Associate
Penn State University
University Park, PA, USA

ABSTRACT

The pericyclic transmission provides the opportunity to vastly impact transmission design in rotorcraft due to its ability to provide exceedingly high reduction ratios in a single stage that would normally require multiple gear stages. This could lead to lighter transmissions with fewer components, increased reliability, efficiency, speed and decreased cost to maintain. While many previous studies have focused upon the gearing within the pericyclic transmission, this work focused on what influences pericyclic geometry, and how changes in geometry impact bearing loads. Specifically, the loading of bearings that must deliver power from the input shaft to the nutating and rotating gears of the system were of primary concern. A comprehensive look at dynamic loads generated by nutating bodies was performed. Methods to address these dynamic loads via application of counterbalances, and deviation from conventional pericyclic transmission designs were utilized to negate the dynamic moment of concern. Counterbalances negating the dynamic moment were shown to weigh between 30-50% of the pericyclic motion converter gears in a 40:1 reduction ratio pericyclic design at 12,000 rpm input speed and reduced applied moments by three orders of magnitude. Finally, a static solver was used to determine the bearing loads with updated component geometries and mass moment of inertias that included the required counterbalances.

INTRODUCTION

Rigorous goals have been set for improvements in efficiency, reliability, maintainability, range, and speed in future rotorcraft. In order to attain these goals, new innovative configurations and materials must be incorporated into designs that can expand operational envelopes of rotorcraft. One candidate for exploration to meet future vertical lift goals is the pericyclic transmission system. A primary characteristic that separates the pericyclic transmission from conventional gear trains is the utilization of nutational motion in geared bodies, specifically in the motion of the pericyclic motion converter (PMC) gear body. This motion enables the use of gear train geometries that contain highly conformal pitch cones leading to many gear teeth in mesh simultaneously sharing transmission loads. Load sharing enabled by the conformal geometry can lead to quieter transmissions, as well as opportunities for high reduction ratios(~50:1) and an overall higher power density transmission.

The pericyclic drive is composed of four primary components, (1) an input carrier or shaft which drives the (2) PMC body through the PMC bearings, and meshes with (3) the reaction control member (RCM) gear and drives (4) the output gear and shaft. These four components are seen in Figure 1. The input to the drive is either internal (shaft) or external (carrier) to the PMC gears. The RCM gear can be driven by a secondary input to vary the reduction ratio or held stationary to provide the necessary reaction force for the PMC to mesh with the output gear. The transmission can make use of its symmetry to mirror its components and split the drive load through two PMCs, which decreases loads on the input and output due to balancing forces. This symmetry is shown in Figure 1.

Previous bodies of work developed a strong fundamental understanding of the opportunity to make use of nutational motion in mechanical transmissions [1-5]. Kinematics, application of face gears, power flow, and variable speed configurations were investigated further by Elmoznino and Saribay in recent years [6-10]. This further developed designs of the transmission, examined lubrication of conjugate face
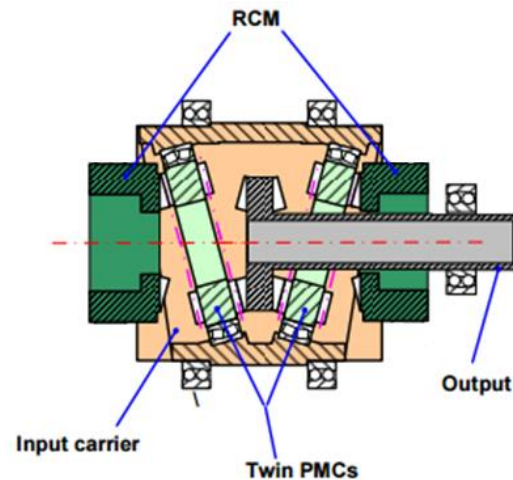

Figure 1. Dual PMC pericyclic transmission with external input carrier driving PMC gears

gears, and highlighted the opportunity to make use of the transmission in rotorcraft applications. Further work by Mathur [11-13] examined the ability to make use of bevel gears in pericyclic transmissions, and further resolved load distribution, mesh stiffness, transmission error and elastohydrodynamic lubrication (EHL) analysis. To this point, understanding of meshing gear faces is fairly well understood. A full model of the pericyclic transmission, including all bearings and geared bodies, has yet to be developed. Application of such tools will be critical to fully understanding loading of and sizing of individual transmission components.

One component in particular, the PMC bearings which are visible in Figure 2, are of particular design concern. Previous work dealing with the dynamics of a geared nutating plate body dating back to the 1970's [14] showed that bearing loads due to the dynamic moment generated, in their particular case, would be roughly 28 times greater than the loads due to the gear reaction forces. While PMC bearing loads had been investigated briefly in previous published work related to the pericyclic transmission, they neglected this critical dynamic moment term. This led to a desire to fully appreciate the dynamic moments generated by the PMC body and translate them to radial forces acting upon the PMC bearings. This work seeks to define the expected static and dynamic moments the PMC bearings must contend with, as well as reveal the resulting radial loads associated with these moments. The design space of the Pericyclic transmission, more specifically the PMC, will also be explored to reveal what factors heavily impact geometry and kinematics, and subsequently dynamics and bearing loads.

PMC GEOMETRY AND POWER FLOW

PMC Pitch Cone Geometry

For pericyclic transmissions utilizing internal and external bevel gears, the geometry of the transmission is largely driven by the pitch cone angles and pitch diameters. These pitch cone angles define the shape of the meshing gear faces of the three geared bodies: the stationary RCM, the rotating and nutating PMC, and the output gear. The PMC geometry is especially sensitive to the pitch cone angles due to its two internal bevel gear faces providing bounds to the body and defining its size.
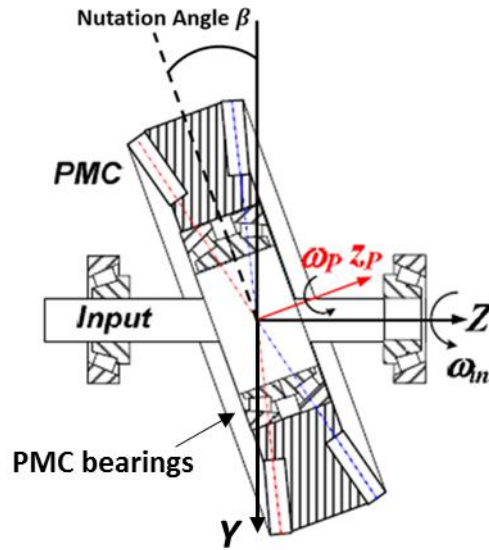
Figure 2. PMC and input shaft cutaway displaying location of PMC bearings

The pitch cone apexes across all geared members are required to be coincident for the gears to mesh properly, and the point where they coincide is the nutation and rotation center of the PMC. Figure 3 displays the meshing of the PMC with the RCM and Output gear bodies as well as the coincidence of the two PMC pitch cone vertices.

The pitch cone angles of these three bodies are mathematically defined by five parameters, the teeth numbers of each gear pair where N1 denotes the RCM gear, N2 the PMC face meshing with the RCM, N3 the PMC face meshing with the output, and N4 for the output gear. The fifth defining parameter is the nutation angle β visible in Figure 2. The corresponding pitch cone angles can then be calculated using:

$$\beta_1 = \text{atan}\left(\frac{\sin(\pi - \beta)}{\left(\frac{N2}{N1}\right) + \cos(\pi - \beta)}\right) \tag{1a}$$
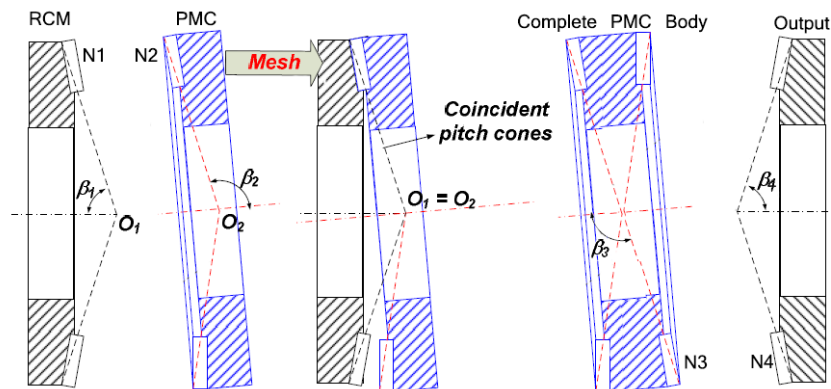
Figure 3. Pericyclic pitch cones and meshing of back to back pitch cones on PMC body with RCM and output

$$\beta_2 = \pi - \beta - \beta_1 \tag{1b}$$

$$\beta_3 = atan\left(\frac{\sin(\pi - \beta)}{\left(\frac{N4}{N3}\right) + \cos(\pi - \beta)}\right) \tag{1c}$$

$$\beta_4 = \pi - \beta - \beta_3 \tag{1d}$$

The corresponding gear mesh pitch diameters are found by multiplying the teeth numbers of each gear by the module, with each meshing gear pair must have the same module value.

Using these equations, impacts of varying parameters allows for changes in geometry to be observed. In particular, variation in nutation angle is a good candidate to examine as it impacts all pitch cone angles while not changing the overall reduction ratio of the transmission system. This ratio is defined as:

$$\frac{\omega_{in}}{\omega_{out}} = \frac{1}{\left(1 - \frac{N1}{N2} * \frac{N3}{N4}\right)} \tag{2}$$

A common tooth number set provided by Ref. 11 uses an N1, N2, N3, and N4 of 52, 54, 81, and 80, which provides a reduction ratio of 40:1. A module of 1/6 in/teeth for both gear sets, also used in previous studies, was used to generate pitch diameters. Using these parameters and Equation 1, pitch cone angles with varying nutation angle from two degrees to eight degrees were generated and plotted to study impacts on PMC geometry. Figure 4 below displays the pitch cones as nutation angle varies, the most obvious trend that is observed is the flattening of the PMC axially as the nutation angle increases. The dramatic decrease in length is accompanied by a peeling of the internal bevel gear faces away from the external bevel gear faces on the RCM and output gear. This decreases the conformity of the gear meshes as well as the number of teeth simultaneously in contact, removing the beneficial load sharing and quiet operation of the transmission. The axial shortening of the PMC body also has the critical effect of
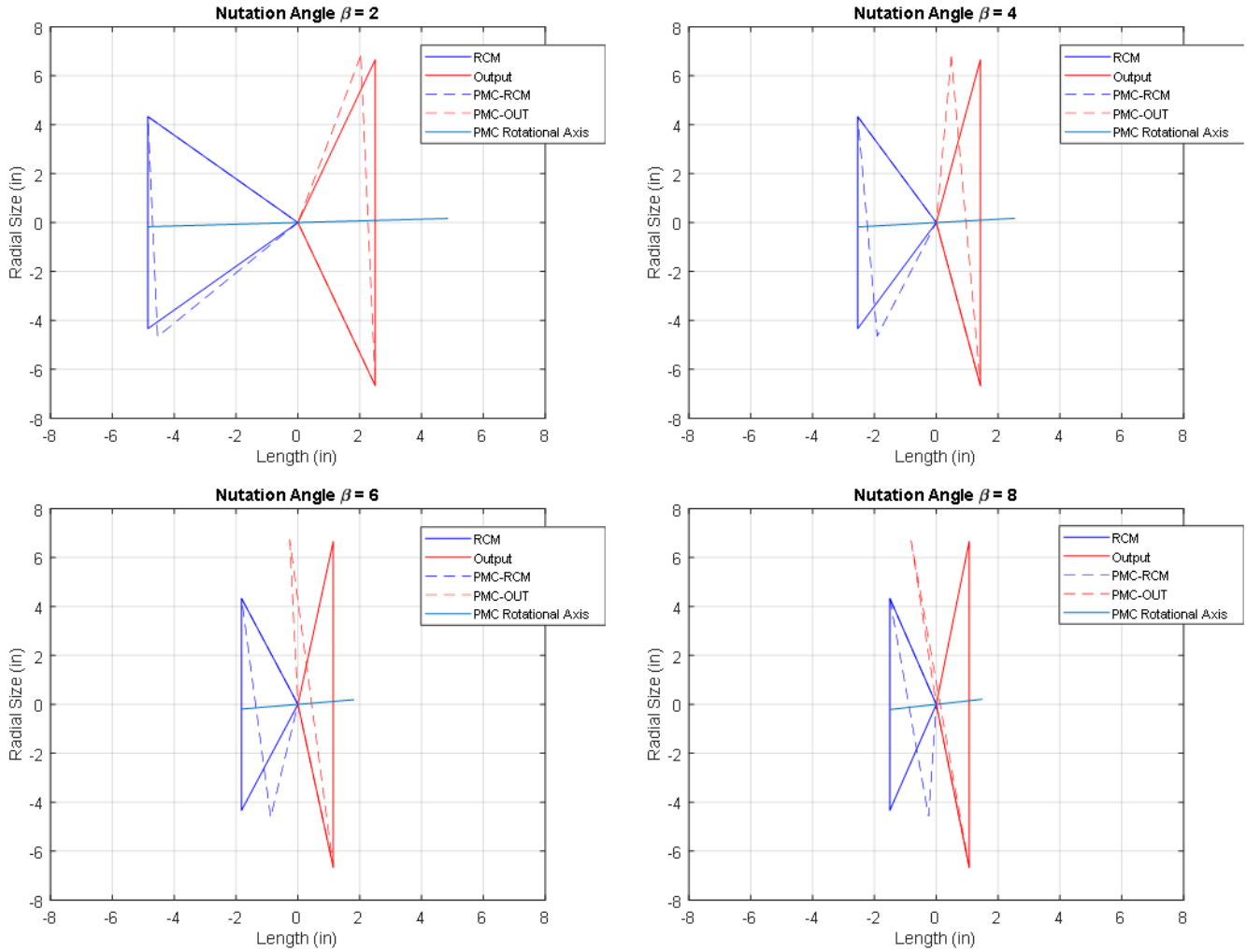

Figure 4. Pericyclic pitch cone shapes with varying nutation angle displaying reduction of total length through flattening of PMC body

3

limiting the area available for the PMC bearings which drive power from the input shaft or carrier to the PMC. Additionally, the decreased length limits the effective lever arm with which the PMC bearings radial forces react the input carrier torque in the direction of the nutational velocity component. This effect will be touched on in the coming section. One positive impact that comes with increased nutation angle is the flattening of the PMC pitch cones greatly decreases the overall size, and therefore weight, of the PMC body. Mass efficiency is critical for airworthiness of rotorcraft transmission components, so while the negative impacts of increased nutation angle are notable, the ability to greatly cut weight of the transmission cannot be ignored.

Beyond these low nutation angles presented in Figure 4 it must be noted that for a given pericyclic geometry there will be a point at which the pitch cone angles of one of the PMC gear faces will invert from internal to external pitch cones. The PMC output gear side at eight degree nutation angle is on the verge of this inversion. If the angle is increased beyond the point of inversion, the transmission ceases to function as a pericyclic transmission and behaves as a humpage drive. This design space will not be explored within this work due to the interest to focus mainly on the pericyclic transmission system architecture.

Input Power and Torque Transfer to PMC

In order to understand the manner in which power is transmitted from the input to the PMC through the PMC bearings, the velocity components of the PMC must be found. The input rotational velocity is given as:

$$\overrightarrow{\Omega_{in}} = \begin{Bmatrix} 0 \\ 0 \\ \omega_{in} \end{Bmatrix} \tag{3}$$

The angular velocity components of the input collars on which the PMC bearings sit can then be found through a rotation about the x axis by the nutation angle β:

$$R_x = \begin{bmatrix} 1 & 0 & 0 \\ 0 & \cos(\beta) & -\sin(\beta) \\ 0 & \sin(\beta) & \cos(\beta) \end{bmatrix} \tag{4}$$

such that:

$$\vec{\Omega}_{in} = \begin{bmatrix} 1 & 0 & 0 \\ 0 & \cos(\beta) & -\sin(\beta) \\ 0 & \sin(\beta) & \cos(\beta) \end{bmatrix} \cdot \begin{Bmatrix} 0 \\ 0 \\ \omega_{in} \end{Bmatrix} \\ = \begin{Bmatrix} 0 \\ -\omega_{in} * \sin(\beta) \\ \omega_{in} * \cos(\beta) \end{Bmatrix} \tag{5}$$

The PMC speed can then be represented as a combination of the input shaft collar speed and the gear ratio between the

RCM and PMC gear. Ref. 9 discusses this in depth and the PMC angular velocity is shown as:

$$\vec{\Omega}_{PMC} = \begin{Bmatrix} 0 \\ -\omega_{in} * \sin(\beta) \\ \omega_{in} * \cos(\beta) - \omega_{in} * \left(\frac{N1}{N2}\right) \end{Bmatrix} \tag{6}$$

With angular velocities of the input and PMC bodies understood, torque transfer from the input to the PMC is calculable. Torque cannot be transferred through bearings in the direction in which they rotate, which is the direction of the PMC rotational velocity. Through conservation of energy, the input power driving torque into the PMC must come from the nutational velocity component of PMC motion: $-\omega_{in} * \sin(\beta)$. The torque from the input carrier to the PMC can then be described as the input power divided by the nutational speed of the PMC body. A generalized form of this is laid out in equations for epicyclic drive trains in Ref. 5 and in this work is described as:

$$\vec{T}_{PMC} = -P_{in} / (-\omega_{in} * \sin(\beta)) \tag{7}$$

with P_{in} as the input power to the transmission.

Due to the nutation angle being somewhere in the range of 2 to 8 degrees, $\sin(\beta)$ is quite low in value and leads to a low nutational angular velocity even with high transmission input speeds. This means the torque from the input carrier to the PMC can remain high even when the transmission operates at high speeds. Through Figure 4 it is understood that increasing nutation angle decreases PMC axial length. This decreases the available distance to place the PMC bearings from the PMC center, limiting the available torque reaction arm. As a result, varying nutation angle allows for a balance between the available torque rection arm, and overall torque due to the PMC nutation speed. Management of these two terms allows for geometries capable of limit static PMC bearing radial loads. There is still the question of how this torque from the input to the PMC compares to the dynamic moments generated by the motion of the PMC body. This will be resolved in the next section with the angular velocity terms derived above.

PMC DYNAMICS

Dynamic Moment Generated by PMC Body

This section will show the dynamic moment generated by the motion of the PMC body. It will be assumed in this section that the mass moment of inertia is symmetrical about the rotation axis of the PMC and is calculated as:

$$I_{PMC} = \begin{bmatrix} I_{pxx} & 0 & 0 \\ 0 & I_{pyy} & 0 \\ 0 & 0 & I_{pzz} \end{bmatrix} \quad (8)$$

The angular momentum is calculated by the dot product of the moment of inertia and the angular velocity of the PMC body from Equation 6:

$$\vec{H}_{PMC} = I_{PMC} \cdot \vec{\Omega}_{PMC}$$
$$= \begin{bmatrix} 0 \\ -I_{pyy} * \omega_{in} * \sin(\beta) \\ I_{pzz} * \left(\omega_{in} * \cos(\beta) - \omega_{in} * \left(\frac{N1}{N2} \right) \right) \end{bmatrix} \quad (9)$$

The dynamic moment is calculated through the time rate of change of the angular momentum:

$$\frac{D\vec{H}_{PMC}}{Dt} = \frac{\delta \vec{H}_{PMC}}{\delta t} + \vec{\Omega}_{PMCf} \times \vec{H}_{PMC} \quad (10)$$

In this study it is assumed that the time derivative of the change in angular momentum is zero due to the assumed operation of the pericyclic transmission at a fixed speed and $\vec{\Omega}_{PMCf}$ is the angular velocity of the PMC frame described in Equation 5. A reorganized form of the term resulting from the cross product is shown as:

$$\frac{D\vec{H}_{PMC}}{Dt}$$
$$= \begin{bmatrix} -\omega_{in}^2 * \sin(\beta) * [I_{pzz} * \left(\cos(\beta) - \left(\frac{N1}{N2} \right) \right) - I_{pyy} * \cos(\beta)] \\ 0 \\ 0 \end{bmatrix} \quad (11)$$

It was also assumed that the inertial body of the PMC is in the shape of a hollow cylinder with a mass M, inner radius R_i, an outer radius R_o, and some length L. Centering this symmetrical cylinder at the nutation point of the PMC, the inertia terms are approximately written as:

$$I_{pxx} = I_{pyy} = \frac{1}{4} * M * (R_O^2 + R_i^2) + \frac{1}{12} * M * L^2$$
$$I_{pzz} = \frac{1}{2} * M * (R_O^2 + R_i^2) \quad (12)$$

Using tooth numbers to generate lengths and radii from the calculated pitch cone angles in Figure 4 the dynamic moment was calculated. Assuming that R_o is the outer radius of the larger of the two PMC pitch cones, R_i is the outer radius of the smaller of the two, and estimating the total length is symmetrical about the PMC nutation center the moment of inertia is found. The mass of the PMC is found by using the density of gear steel (0.2908 lbs/in^3) times the volume of a

hollow cylinder. For this example we can use a configuration utilized by previous work of rotorcraft transmission of 1000 HP with an input speed of 12,000 rpm and with a reduction ratio of 40:1 resulting in an output speed of 300 rpm. This study focuses on a dual pericyclic configuration where two PMC bodies are assumed to equally share the power from the input. The resulting dynamic moment from two to eight degrees nutation angle for one of the PMC's is plotted on a log scale in Figure 5 along with the static torque delivered from input carrier to the PMC through the PMC bearings as was discussed in the previous section. The dynamic moments calculated through this approach are roughly three orders of magnitude greater than the static torque shown and are immediately seen as a critical issue for operation of the transmission at high speeds. These values are notably higher than the cited work which showed only two orders of magnitude higher dynamic loads than static loads. This is partially due to the high operation speeds desired for case study. It is also due in part to the lack of mass optimization of the PMC body through tooth number selection and nutation angle.

Without any additional attempts to diminish the dynamic moment generated, many designs of the pericyclic transmission are severely speed limited. Decreasing the input speed is the simplest way to examine where the dynamic moment is on the same order of magnitude as the input torque. This is depicted in Figure 6 where the input speed is dropped until the orders of magnitude of the moments are similar to one another. It isn't until the Input speed is around one order of magnitude lower that the two moments are equal in value. At an input speed of 1,000 rpm this design's 40:1 reduction ratio would provide an output speed of 25 rpm, far too slow for use in rotorcraft. It was determined that a method to
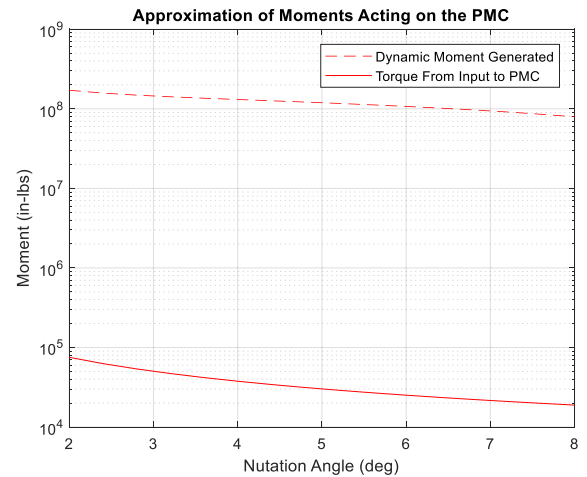

Figure 5. Dynamic moment of PMC in comparison with input moment delivered to PMC

reduce or eliminate the dynamic moment was required to make the pericyclic drive feasible.
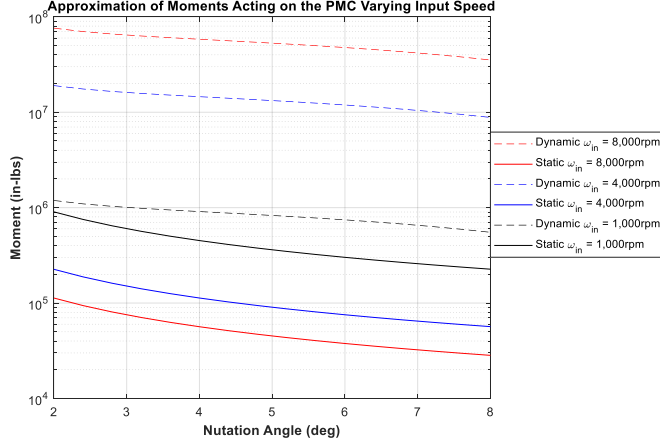
Examination of Dynamic Moment Terms

Figure 6. Dynamic moment and input torque for several transmission input speeds

The dynamic moment generated by the body is composed of two primary terms, the first related to the mass moment of inertia about the rotational axis and the second related to the mass moment of inertia about the nutational axis.

$$M_D = -\omega_{in}{}^2 * \sin(\beta) * [I_{pzz} * \left(\cos(\beta) - \left(\frac{N1}{N2}\right)\right) - I_{pyy} * \cos(\beta)] \tag{13}$$

Setting the dynamic moment term equal to zero, a condition could be discovered with which the dynamic moment could be neutralized. Dividing out the sine of the nutation angle and the input speed squared provides:

$$0 = I_{pzz} * \left(\cos(\beta) - \left(\frac{N1}{N2}\right)\right) - I_{pyy} * \cos(\beta) \tag{14}$$

From this equation it is observed that the dynamic moment cancellation is independent of transmission input speed. Additionally, due to the two terms being subtracted from one another, a scenario could be found in which the two terms are equal, leading to a cancellation of the dynamic moment. Terms were rearranged to help better visualize necessary steps to cancel the dynamic moment. One way to display Equation 14 was as equivalent ratios of nutation angle and tooth number terms, and inertial terms:

$$\frac{I_{pyy}}{I_{pzz}} = \left(\cos(\beta) - \left(\frac{N1}{N2}\right)\right)\Big/ \cos(\beta) \tag{15}$$

This ratio is helpful and will be discussed further later, it doesn't provide much insight to what the appropriate tooth numbers or nutation angles should be. To get a better idea of mathematically what design aspects are required, the approximate mass moment of inertia terms for a PMC body from Equation 12 were substituted into Equation 14 so that:

$$\frac{1}{2} * M * (R_O^2 + R_i^2) * \left(\cos(\beta) - \left(\frac{N1}{N2}\right)\right) - \left(\frac{1}{4} * M * (R_O^2 + R_i^2) + \frac{1}{12} * M * L^2\right) * \cos(\beta) = 0 \tag{16}$$

Solving for $\frac{N1}{N2}$ results in the equation:

$$\frac{N1}{N2} = \frac{1}{2} * \cos(\beta) - \frac{1}{6} * \frac{\cos(\beta)L^2}{(R_O^2 + R_i^2)} \tag{17}$$

Upon examination of this formula it is difficult to see a clear trend that aids in diminishing the dynamic moment. One option is to increase the effective magnitude of the $(R_O^2 + R_i^2)$ term by adding additional weight at the nutation center without increasing the effective axial length L that mass's moment of inertia would act at via a counterbalance, you could make

$$(R_O^2 + R_i^2) \gg L^2 \tag{18}$$

If this were the case then $\frac{L^2}{(R_O^2 + R_i^2)}$ would be near zero, leaving the right side of Equation 17 with only the one half cosine of the nutation angle. Knowing that the nutation angle must be a relatively low value, it could be assumed that $\cos(\beta)$ would be a value near one. This leaves us with the desire to have $\frac{N1}{N2}$ to be roughly less than or equal to one half to nearly eliminate the dynamic moment generated.

There are two major impacts on pericyclic desing space with having $\frac{N1}{N2} \leq \frac{1}{2}$. The first noticeable impact this restraint would have is on the reduction ratio of the transmission. It would limit the high reduction ratios achieved by having very

close tooth numbers in meshing gear faces, like in the first example, due to the reduction ratio approximately equaling:

$$\frac{\omega_{in}}{\omega_{out}} \approx \frac{1}{\left(1 - \frac{1}{2} * \frac{N3}{N4}\right)} \tag{19}$$

so that even when $\frac{N3}{N4}$ was close together in tooth number and approximately one the reduction ratio would only be around 2:1. In order to obtain higher reduction ratios which make the pericyclic competitive, the tooth difference in the second gear mesh would also have to increase. For example, in order to obtain the 40:1 reduction ratio in the previously stated example, $\frac{N3}{N4}$ would need to be an integer multiple of $\frac{39}{20}$. Higher variation in tooth number needed for higher reduction ratios between meshing gear faces would also lead to a much less conformal gear mesh, decreasing the number of teeth simultaneously in contact and increasing tooth loads.

The second noticeable impact on transmission design from a configuration fixing $\frac{N1}{N2} \leq \frac{1}{2}$ is in sizing of components. For example let us consider a 40:1 reduction ratio pericyclic transmission once again with similar PMC tooth numbers to the first example but with the RCM and output (N1 and N4) tooth numbers altered to satisfy the constraint that $\frac{N1}{N2} \leq \frac{1}{2}$. Gear teeth numbers of 20, 50, 78, and 32 were chosen for N1, N2, N3 and N4 respectively. Pitch cone sizes were calculated once again using Equation 1, and instead of plotting pitch cone geometries, due to their odd shapes, plotting the PMC axial length across the varying nutation angles was easier and is shown in Figure 7 along with lines depicting the approximate PMC inner and outer radius defined by the two pitch cone diameters. Figure 8 displays the inertial ratios mentioned in Equation 15 and Figure 9 a pitch cone sample output where overall PMC length is more reasonable at a higher nutation angle. The range of nutation angles the PMC size was examined across was much larger than the previous example. This is due to the large difference in tooth number increasing the inflection point of the pitch cones to much greater nutation angles. It should be noted that increasing the range of the nutation angle is beneficial to the static PMC bearings loads. As discussed earlier, increased nutation angle increases the nutational velocity component, which decreases the torque delivered from the input carrier to the PMC which must pass through the PMC bearings. This is beneficial in decreasing maximum bearing loads.

From Figure 8 the two inertial terms converge at higher nutation angles. At low nutation angles the terms are more difficult to balance due to the long length of the PMC greatly increasing the inertial term in the direction of nutational motion, I_{pyy}, driving up the ratio of the two moments of inertia. As the nutation angle increases, length decreases, reducing the ratio of the inertial terms. This high nutation angle regime provides an opportunity to reasonably

counterbalance the PMC to eliminate the dynamic moment generated and will be utilized in the next section. It is clear
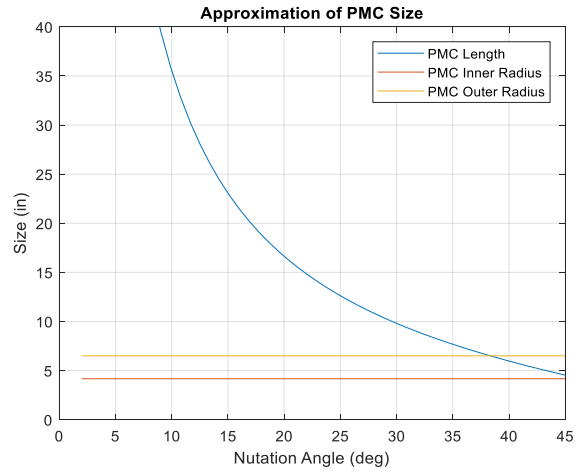

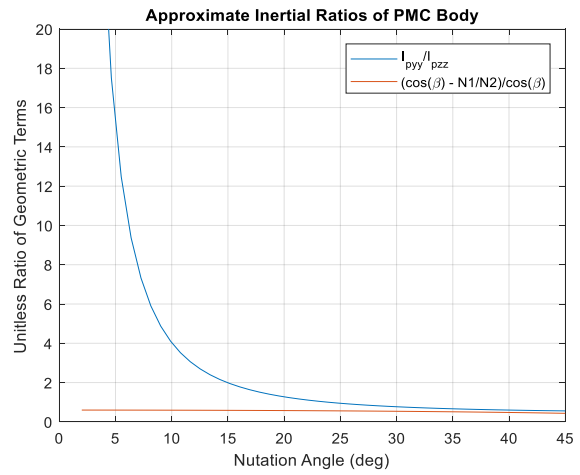**Figure 7. PMC approximate size across varying nutation angles**

Figure 8. PMC inertial ratio and geometric ratio require to be equivalent for dynamic moment cancellation
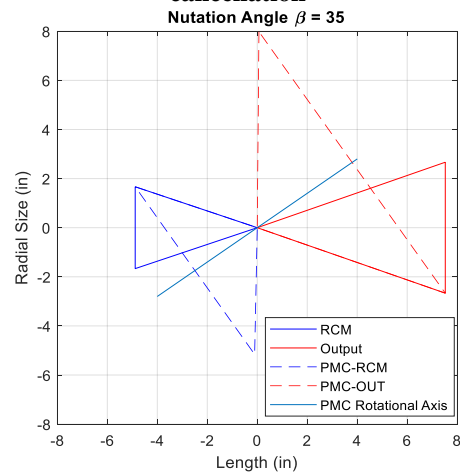

Figure 9. Example PMC geometry at high nutation angle and high difference in meshing gear tooth numbers

7

that it is possible to generate PMC geometries with high differences in tooth number and under the constraint $\frac{N1}{N2} \leq \frac{1}{2}$, but to provide reasonable solutions much higher nutation angles are required.

Addition of Counterbalance to PMC to Negate Dynamic Moment

As discussed in the previous section it was desired to provide a counterbalance to the PMC that would be capable of altering the mass moment of inertia terms so that $(R_O^2 + R_i^2) \gg L^2$ subject to certain tooth number constraints. Geometry largely drives the ability to counterbalance the PMC. In order to accurately develop a counterbalance a more accurate representation of the PMC mass moment of inertia terms based upon pitch cone geometry was needed. To accomplish this, the PMC body was split into three sections that varied in size based on pitch cone geometry and represented the sections of the PMC with the gear face width taken into account. These generalized sections are shown in Figure 10. Solid lines denote the PMC body and are numbered one to three along with a full cutaway image of a PMC body showing the pitch cone angles, pitch diameters, and gear tooth face widths mark FW1 and FW2.
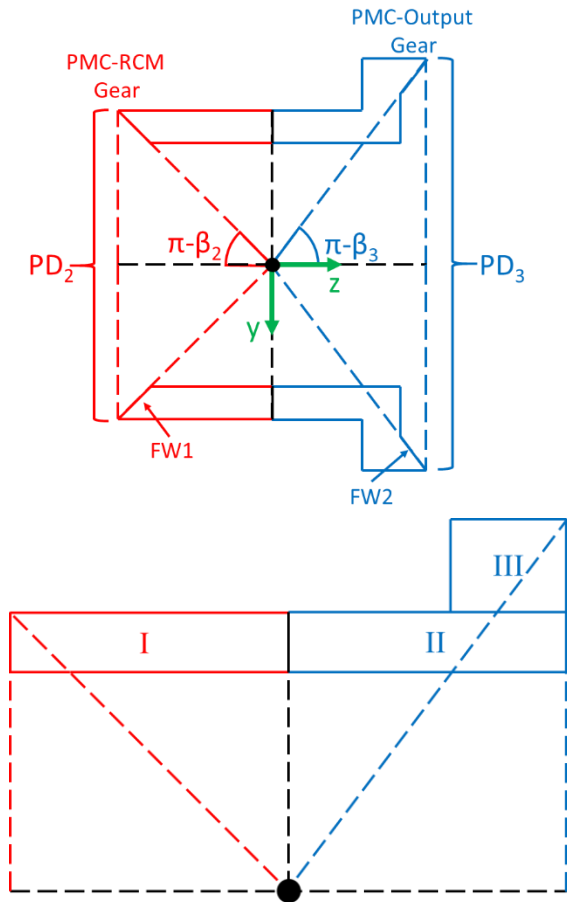
With a more realistic inertial body generated, mass moments of inertia can once again be found for a PMC body now with some assumed counterbalance term included that impacts the overall mass moment of inertia:

$$I_{PMC} = \begin{bmatrix} I_{xx} + I_{cbxx} & 0 & 0 \\ 0 & I_{yy} + I_{cbyy} & 0 \\ 0 & 0 & I_{zz} + I_{cbzz} \end{bmatrix} \quad (20)$$

with the terms denoted by a cb belonging to the PMC counterbalance. Based on Figure 8, we know that the counterbalance must increase I_{pzz} with respect to I_{pyy}, in addition it is assumed the geometry of the counterbalance must be some axisymmetric shape. It was decided that a hollow cylinder centered about the nutation point would be used, of which the inner radius, R_i, the outer radius, R_o, and the length, L, could be altered. To balance the PMC, the shape of this cylinder would need a large inner and outer radius to increase I_{pzz} and a short length as to not increase I_{pyy} significantly. Figure 11 depicts a diagram of what this counterbalance would roughly look like in location and with regards to the PMC body as well as its defining geometry parameters.

It was desired for the mass of the counterbalance to be as low as possible while still altering the mass moment of inertia sufficiently to eliminate the dynamic moment generated through alteration of its inner radius, outer radius, and length. This lead to the development of a tool in Matlab that sought to minimize counterbalance mass while providing the nonlinear constraint that the dynamic moment was equal to zero. Additional constraints made sure the outer radius of the counterbalance was greater than the inner radius, and the
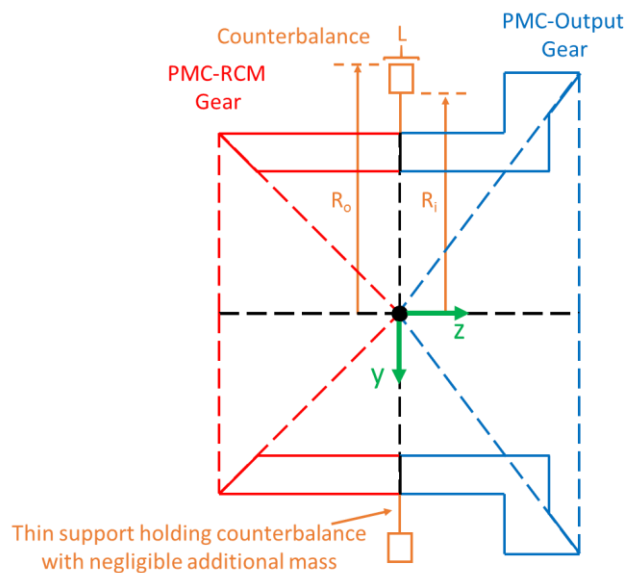

Figure 10. PMC body inertial body showing nutation angles, dimensions, and close-up of inertial subcomponents

Figure 11. PMC body with counterbalance attachment and dimensions shown

inner radius of the counterbalance had to be outside of the PMC as to not impact the internal space for bearings.

A test case was run to determine if the tool could provide geometries that were capable of balancing the PMC body. The previous example of teeth numbers (20, 50, 78 and 32) were used to maintain the constraint that $\frac{N1}{N2} \leq \frac{1}{2}$ and provide a reduction ratio of 40:1. The face widths of the gears were set at one inch and the minimum length of the counterbalance was restricted to one inch as well. The minimum limit on the difference between inner and outer radius was set at 1 in. The radii of the counterbalance were allowed to have a max value of 500 inches to attempt to achieve full dynamic moment elimination. An upper limit of 500 inches radius is unrealistic but was require to numerically find solutions at lower nutation angles. The tool was executed and produced inner radii, outer radii, and total lengths across a range of nutation angles for the counterbalance that generated zero dynamic moment. The geometry results for the counterbalance are plotted in Figure 12 and the PMC total mass for the three body inertial model and the counterbalance mass is plotted in figure 13. It must be noted that the masses shown are exceedingly high, especially at low nutation angles when the PMC length is unrealistically long. These large masses are due to the generalized PMC body used having no mass optimization. Additionally, gear teeth numbers and face widths also have not been optimized for this configuration.

The counterbalance tool is capable of finding a solution across a wide range of nutation angles. Figure 14 shows that counterbalancing is achieved with only 30-40% of the PMC weight for the majority of nutation angles. The geometry of the counterbalance is a radially large cylinder with a short axial length, as was predicted based on the ratio of inertial terms plotted in Figure 8. The inner radius, in what appears to be all cases, minimizes its distance from the outer radius, and the length remains at its minimum value of one inch across all solutions. A feature to take note of on these plots is the spike in counterbalance weight, and radius around 37 degrees nutation followed by a flat line. Beyond this point the tool is unable to solve for a scenario in which the counterbalance is able to fully negate the dynamic moment generated. The solver defaults to providing a solution of the minimum mass possible for the counterbalance based upon minimum bounds placed on the variables, but no longer negates the dynamic moment. This inability to negate the dynamic moment at higher nutation angles makes sense due to the earlier assumption that for $\frac{N1}{N2} \leq \frac{1}{2}$ to apply, $\cos(\beta)$ had to be near a value of 1. With the increased nutation angle $\cos(\beta)$ strays further from 1, the geometry deviates from the feasible range, and the solver fails. Despite this, it is clear that for a generalized PMC geometry it is possible to sufficiently alter the mass moment of inertia such that the dynamic moment generated is canceled. The counterbalancing can be achieved with less than a 50% increase in PMC mass, limiting additional weight to the transmission. Counterbalancing addresses a critical PMC bearing loading concern raised by
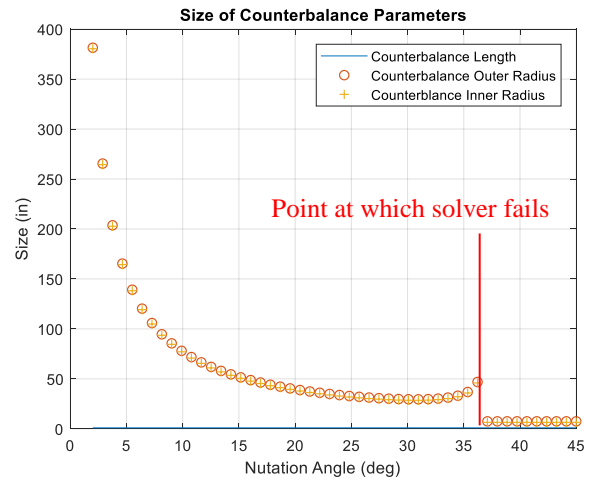

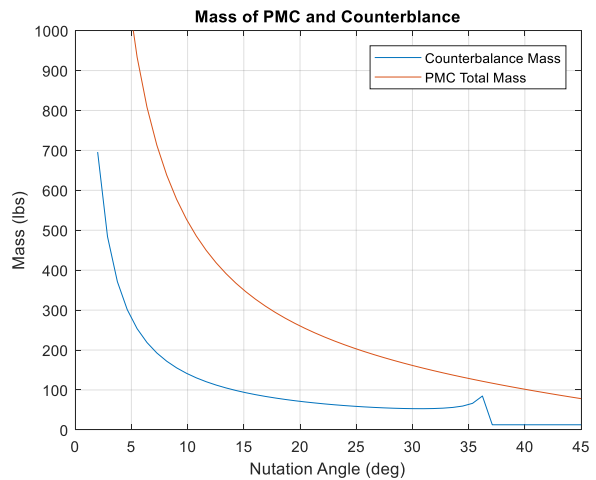**Figure 12. Dimensions of counterbalance required to negate dynamic moment**

Figure 13. Mass of counterbalance with relation to PMC mass
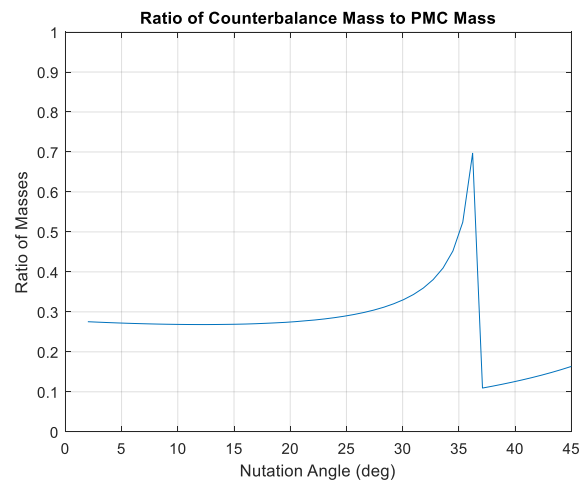

Figure 14. Ratio of counterbalance mass to PMC mass

9

previous authors, and by previous sections of this work. The additional mass achieving this is offset in the reduced mass of the bearings required to manage pericyclic transmission loads.

Centrifugal Force and Moment Due to Offset COG

One additional loading term on the PMC that must be acknowledged is due to centrifugal loads generated when the center of gravity(COG) of the PMC is offset from the PMC nutation center. Due to the tooth difference between the two sides of the PMC and the difference in tooth number of the gears they mesh with, the PMC will inevitably be asymmetrical causing a shift in the COG from the nutation center. This means that the COG will have an orbit about the input's rotational axis at a speed equivalent to the angular velocity of the PMC body times a rotation matrix about the x axis of the PMC by a negative value of the nutation angle.

$$\omega_c = \begin{cases} 0 \\ -\omega_{in} * \sin(\beta) * \cos(\beta) + \sin(\beta) * \omega_{in} * \left(\cos(\beta) - \left(\frac{N1}{N2}\right)\right) \\ \omega_{in} * \sin(\beta) * \sin(\beta) + \cos(\beta) * \omega_{in} * \left(\cos(\beta) - \left(\frac{N1}{N2}\right)\right) \end{cases} \tag{21}$$

Where the rotational component of ω_c, ω_{cz}, is the speed at which the center of gravity is orbiting. This generates a centrifugal force which is depicted in Figure 15 along with the COG orbital path, and is calculated by:

$$F_c = M_{PMC} * \omega_{cz}^2 * d * \sin(\beta) \tag{22}$$

where M_{PMC} is the mass of the PMC, and the term, $d * \sin(\beta)$, is the radius of the orbit path the PMC center of gravity takes. F_c is broken down into an axial and a radial load acting on the PMC body when returned to the PMC frame of reference. The axial load F_{ca} is reacted by PMC axial bearing. The radial load F_{cr}, and resulting moment generated by this radial load and the cross product of the offset distance of the COG, d, from the PMC center, is reacted by the radial bearings.

This centrifugal load is minimized if the COG is aligned with the nutation center. To reduce the COG offset magnitude, and consequentially the centrifugal force generated, a set of gear tooth numbers should be selected which limits the difference in size between the RCM and output side of the PMC. This is highly effective in balancing the two side's masses and further reduces high, speed related, loads applied to the PMC bearings. Tooth numbers in the remainder of this work will be selected such that N2 and N3 are very close in value and any resulting offset COG will be negated via an addition of mass that has negligible impact on the moment of inertia of the PMC.
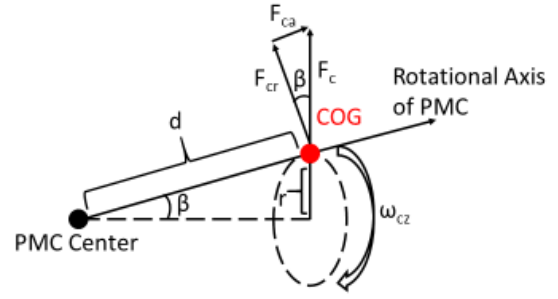

Figure 15. Orbit of PMC offset center of gravity and resulting centrifugal force generated

STATIC MODEL OF DUAL PMC PERICYCLIC TRANSMISSION

With a solution to manage the dynamic load in place, a static solver was built in Matlab that could be used to provide an estimated load for each bearing and gear mesh. The static solver designed was for an internal input shaft driven, fixed RCM, dual PMC pericyclic transmission, a schematic of which is seen in Figure 16. The bodies within the system were assumed to be completely rigid and symmetric, and the gear meshes were modeled as point loads at the center of the gear face widths. It was also assumed that power flowed through the system was split evenly between the two PMCs. Each PMC was assumed to have two bearings, one of which provides a radial support, the other a radial and axial support. The bearings are spaced on either side of the nutation center three quarters of the distance out to the gear mesh on their respective side so that they are wholly within the PMC while taking advantage of a long lever arm. The output body, comprised of the two output gears back to back, and input shaft also have two bearings with the same configuration as the PMC (one reacting to a radial load, and the other reacting to an axial and radial load) with bearings placed symmetrically about their centers. Each radial bearing provides two unknown forces, a reaction force in the x and a reaction force in the y direction of corresponding bodies. Bearings taking on an additional axial load provide an additional unknown reaction force in the z direction for corresponding bodies. For the gear mesh reaction forces, only the magnitude of the tangential force transmitting torque was treated as an unknown. The remaining mesh forces in the x, y and z directions were based upon bevel gear pitch cone geometry. For a single unknown mesh force in vector form, say for the gear mesh force between the first PMC and RCM gear, could be written as:

$$\overrightarrow{F_1} = \begin{cases} f_1 \\ f_1 * \tan(\alpha_1) * \cos(\beta_2) \\ f_1 * \tan(\alpha_1) * \sin(\beta_2) \end{cases} \tag{23}$$

Where f_1 is the unknown tangential force term, α_1 is the pressure angle of the gear mesh, and β_2 is the bevel gear pitch cone angle of the PMC body.
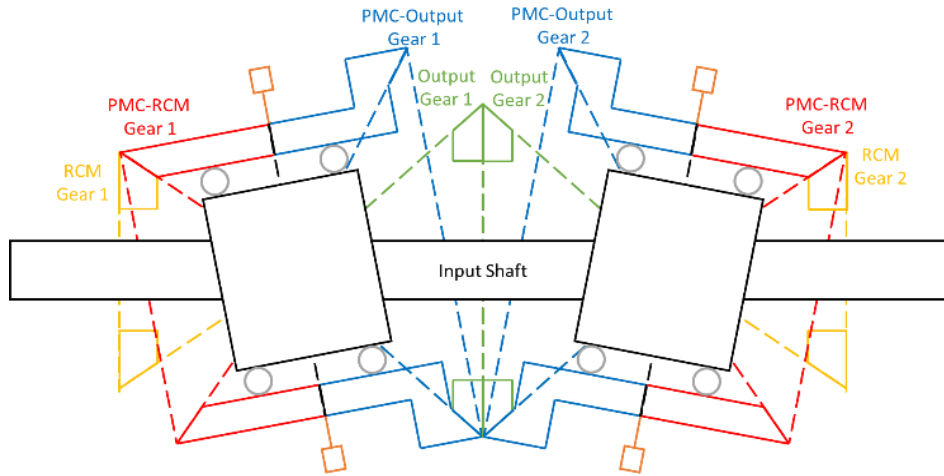
Figure 16. Cutaway view of dual PMC pericyclic with internal input shaft displaying various rigid bodies based upon pitch cone geometry and using circles to depict PMC bearing locations

The 8 bearings in the system provide a total of 20 unknowns, the 4 gear meshes provide an additional 4 unknowns, and the requirement to derive the output torque from the system (input power and torque are selected as desired) adds an additional unknown leading to a total of 25 unknowns to be solved for with 4 bodies. These 4 bodies only provide a total of 6 equations each (3 force summation and 3 moment summations about each body) leading to 24 equations to solve for 25 unknowns. Due to the symmetry in the system and the assumption that power flows evenly, the gear mesh forces on the output bodies are equal and opposite. No net axial force is applied to the output body. While this would not be realistic for a real model of the pericyclic load train due to misalignments and asymmetries creating uneven power flow between the two PMC's, for this basic model to derive bearing load estimates it was determined sufficient. Without a net axial force applied to the output, one unknown is removed from the system. This simplification leads to 24 unknowns to solve for and 24 equations to solve them with making a statically determinate system.

With this static simulation developed, a test case was run using the model. The test case transmission had an input power of 1000 HP and an input speed of 12,000 rpm being driven into the pericyclic drive. Teeth numbers of 30, 75, 78, and 32 were utilized due to the desire to diminish any centrifugal loads by having the smallest difference between N2 and N3 possible while still providing a reduction ratio of 40:1. PMC pitch cone geometries were calculated, inertial bodies were generated, and counterbalance solutions minimizing additional mass were found to diminish the dynamic moment generated for a range of nutation angles. The PMC masses and inertial bodies including a counterbalance were fed into the static solver long with their corresponding geometries and gear mesh force locations and bearing loads were resolved. While the solver output all transmission bearing loads, this paper would like to focus specifically on the PMC bearings load results.

Plotted in Figure 17 are the PMC bearing radial and axial loads for this test case. The first major characteristic to take note of is the sharp rise in radial loads around 37 degrees nutation but the lack of such a feature in the axial loads. As discussed before, this is due to the counterbalance tool being
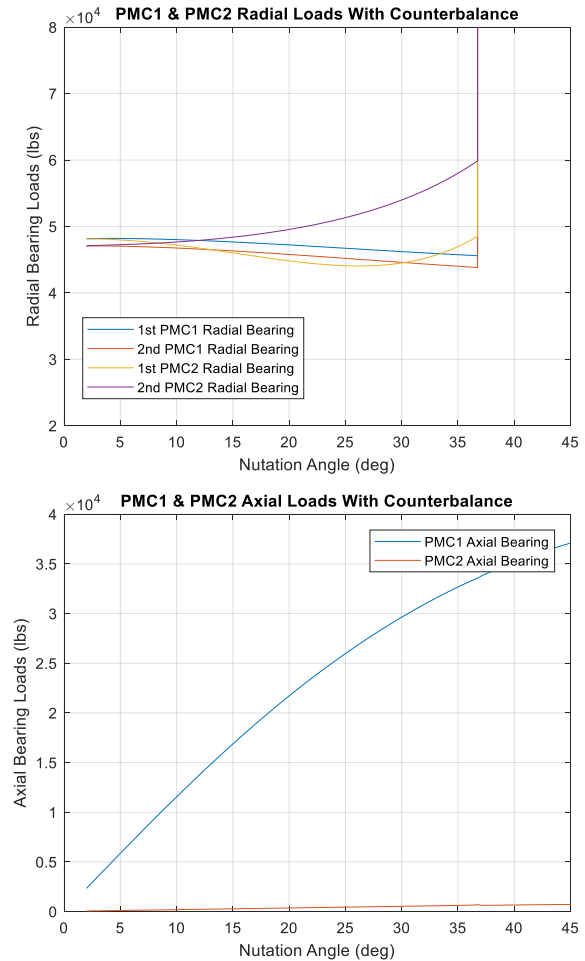

Figure 17. Radial and axial loads on PMC bearings for 1000 HP counterbalanced transmission

unable to balance the PMC beyond a certain nutation angle and the dynamic moment reemerging and driving up PMC radial loads. Due to axial loads being unable to react to the dynamic moment, they do not observe increases in loads with the reemerged dynamic moment. The difference between PMC 1 and PMC 2 in loading trends is due to one input shaft bearing taking on both radial and axial loads, and forcing asymmetry into the PMC loading.

Overall magnitudes of loads are high, but reasonable for the bearing size envelope available. The allowable size of the PMC bearing versus the speed of the bearing is plotted in Figure 18. At 30 degrees nutation angle, the highest radial load for any bearing is approximately 55,000 lbs, its maximum outer diameter is around 11 inches, and it would be required to operate at slightly less than 6,500 rpm. Depending upon bearing type selection, operating speed could be a concern for this particular scenario. In regards with loads, 55,000 lbs is manageable for aerospace grade bearings of this size. Optimization of bodies with regards to mass could decrease overall size of the PMC and counterbalance. In all it was shown that use of counterbalances for the PMC body is an effective means of diminishing exceedingly high bearing loads due to dynamic losses, decreasing bearing losses, and increasing bearing life for an additional mass cost for high speed pericyclic operation.
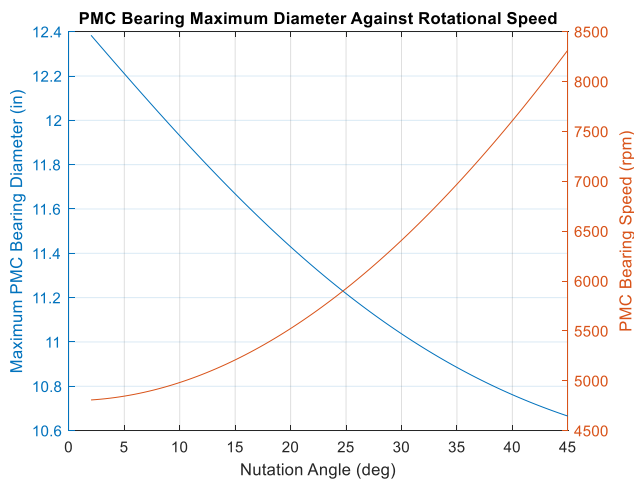

Figure 18. PMC bearing maximum diameter possible for given geometry along with bearing speed

CONCLUSIONS

Within this work the pericyclic design space was explored with a focus on limiting the loading of the PMC bearings. The geometry of the PMC was examined along with the impact of nutation angle on overall size and shape. Angular velocity components of the PMC were developed and the method through which power is delivered from the input to the PMC via the PMC bearings was discussed. The angular velocities were then used to show the expected dynamic loads of the PMC body due to the complex nutation and rotation while moving in and out of mesh. The terms that made up this dynamic load were examined more closely to

determine if there was a discernable method to negate its generation. Tooth number selection was shown to have great impact on the dynamic moment generated due to approximate inertial terms. Inspection of these terms lead to the desire to have $\frac{N1}{N2} \leq \frac{1}{2}$, drastically diverging from conventional tooth number selections. Through this understanding a counterbalancing method was able to be developed and applied that could alter the mass moment of inertia to negate the generation of the dynamic moment. It was shown that for, at most, a 50% increase in PMC weight the dynamic moment of a 40:1 reduction ratio pericyclic could be negated. The possibility of centrifugal loading and its impact on PMC bearings loads was discussed and tooth numbers altered to aid in the balancing of the two halves of the PMC. Finally a static solver was utilized to determine PMC bearing loads in a counterbalanced configuration. Thanks to the removal of the dynamic moment, loads for the given PMC size were found to be within a reasonable range for the PMC bearings. Design space exploration within this paper revealed that tooth numbers and therefore pericyclic transmission design differ greatly when designing for decreased bearing loads as opposed to gear tooth loads. Highly conformal pitch cone geometries attained with low nutation angles and small tooth number differences in mesh, while good for gear design, lead to high dynamic loads when used in rotorcraft designs. Less conformal meshes provide more space for bearings, longer effective lever arms to react to torques, higher nutation angles and nutational speeds decreasing PMC bearing static loads, and a larger design space with which the transmission is counterbalanced reasonably.

Recommendations for future work would include the incorporation of this work that sought to limit critical bearing loads with gear mesh load work so that a balance between load sharing between teeth, and low bearing loads could be found. This work showed that higher nutation angles and less conformal gear pitch cones (causing fewer teeth to be simultaneously in mesh) lead to lower PMC bearing loads. Understanding what type of gear tooth sizes are required to handle the loads associated with these geometries will be a critical design challenge. Higher fidelity geometries and more constraints on transmission design to ensure bodies and shafts are not critically loaded would also be valuable work that would help aid in further maturation and development of the transmission. Finally models that take into account bearing and mesh stiffness would be valuable to examine if deviation from the desired nutation angle would show a significant reemergence of the counterbalanced dynamic moment.

Author contact: Zachary A. Cameron
zachary.a.cameron@nasa.gov
Dr. Edward C. Smith ecs5@engr.psu.edu
Dr. Hans DeSmidt hdesmidt@utk.edu
Dr. Robert C. Bill billrc2@cox.net

ACKNOWLEDGMENTS

REFERENCES

[1]Drago, R., and Lemanski, A., "Nutating Mechanical Transmission," The Boeing Vertol Company, 1974.

[2]Molyneux, W. G., "The Internal Bevel Gear and its Applications," *Journal of Aerospace Engineering*, vol. 211, 1997.

[3] Lemanski, A., and Monahan, T. J., "Non-Traction Pericyclic CVTs," *SAE International,* Vol. 40, 5th ser., 2004.

[4] Nelson, C. A., and Cipra R. J., "Similarity and Equivalence of Nutating Mechanisms to Bevel Epicyclic Gear Trains for Modeling and Analysis," *Journal of Mechanical Design*, vol. 127 pp. 269-277, 2005.

[5] Nelson, C. A., and Cipra R. J., "Simplified Kinematic Analysis of Bevel Epicyclic Gear Trains With Application to Power-Flow and Efficiency Analyses," *Journal of Mechanical Design*, Vol. 127, March 2005, pp. 278-286.

[6]Elmoznino, M., Kazerounian, K., and Lemanski, A. J. , "An Electro-Mechanical Pericyclic CVT (P-CVT)," 12th IFToMM World Congress, Besancon, France, January, 2007.

[7]Elmoznino, M., "The Nature of Power Flow Through the Pericyclic Continuously Variable Transmission," M.Sc. Thesis, University of Connecticut, CT, 2008.

[8]Saribay, Z., "Analytical Investigation of the Pericyclic Variable-Speed Transmission System for Helicopter Main-gearbox", 2009.

[9]Saribay, Z., and Bill, R., "Design Analysis of Pericyclic Mechanical Transmission System," *Mechanism and Machine Theory*, vol. 61, pp. 102-122, 2012.

[10]Saribay, Z., Bill, R., Smith, E., and Rao, S., "Elastohydrodynamic Lubrication Analysis of Conjugate Meshing Face Gear Pairs," *Journal of the American Helicopter Society*, 2012.

[11]Mathur, T., Saribay, Z., Bill, R., Smith, E., and DeSmidt, H., "Analysis of Pericyclic Mechanical Transmission with Straight Bevel Gears," *56th AIAA/ASCE/AHS/ASC Structures, Structural Dynamics, and Materials Conference*, January, 2015.

[12]Mathur, T., Smith, E., DeSmidt, H., and Bill, R., "Load Distribution and Mesh Stiffness Analysis of an Internal-External Bevel Gear Pair in a Pericyclic Drive," American Helicopter Society 73rd Annual Forum Proceedings, Fort Worth, TX, May, 2017.

[13]Mathur, T., Smith, E., Chang, L., and Bill, R., "Contact Mechanics and Elasto-Hydrodynamic Lubrication Analysis of Internal-External Straight Bevel Gear Mesh in a Pericyclic Drive," ASME International Power Transmission and Gearing Conference (PTG), Cleveland, OH, August, 2017.

[14] Anderson, W. J., "Analysis of the Dynamics of a Nutating Body," NASA TN D-7569, 1974.